Scaling of particle and transverse energy production in ^{208}Pb+^{208}Pb collisions at 158·A GeV

The WA98 Collaboration

M.M. Aggarwal[1], A. Agnihotri[2], Z. Ahammed[3], A.L.S. Angelis[4], V. Antonenko[5], V. Arefiev[6], V. Astakhov[6], V. Avdeitchikov[6], T.C. Awes[7], P.V.K.S. Baba[8], S.K. Badyal[8], A. Baldine[6], L. Barabach[6], C. Barlag[9], S. Bathe[9], B. Batiounia[6], T. Bernier[10], K.B. Bhalla[2], V.S. Bhatia[1], C. Blume[9], E.-M. Bohne[9], Z.K. Böröcz[9], D. Bucher[9], A. Buijs[12], H. Büsching[9], L. Carlen[13], V. Chalyshev[6], S. Chattopadhyay[3], R. Cherbatchev[5], T. Chujo[14], A. Claussen[9], A.C. Das[3], M.P. Decowski[18], H. Delagrange[10], V. Djordjadze[6], P. Donni[4], I. Doubovik[5], S. Dutt[8], M.R. Dutta Majumdar[3], K. El Chenawi[13], S. Eliseev[15], K. Enosawa[14], P. Foka[4], S. Fokin[5], V. Frolov[6], M.S. Ganti[3], S. Garpman[13], O. Gavrishchuk[6], F.J.M. Geurts[12], T.K. Ghosh[16], R. Glasow[9], S. K.Gupta[2], B. Guskov[6], H. Å.Gustafsson[13], H. H.Gutbrod[10], R. Higuchi[14], I. Hrivnacova[15], M. Ippolitov[5], H. Kalechofsky[4], R. Kamermans[12], K.-H. Kampert[9], K. Karadjev[5], K. Karpio[17], S. Kato[14], S. Kees[9], H. Kim[7], B. W. Kolb[11], I. Kosarev[6], I. Koutcheryaev[5], T. Krümpel[9], A. Kugler[15], P. Kulinich[18], M. Kurata[14], K. Kurita[14], N. Kuzmin[6], I. Langbein[11], A. Lebedev[5], Y.Y. Lee[11], H. Löhner[16], L. Luquin[10], D.P. Mahapatra[19], V. Manko[5], M. Martin[4], G. Martínez[10], A. Maximov[6], R. Mehdiyev[6], G. Mgebrichvili[5], Y. Miake[14], D. Mikhalev[6], Md.F. Mir[8], G.C. Mishra[19], Y. Miyamoto[14], B. Mohanty[19], M. J. Mora[10], D. Morrison[20], D. S. Mukhopadhyay[3], V. Myalkovski[6], H. Naef[4], B. K. Nandi[19], S. K. Nayak[10], T. K. Nayak[3], S. Neumaier[11], A. Nianine[5], V. Nikitine[6], S. Nikolaev[6], P. Nilsson[13], S. Nishimura[14], P. Nomokonov[6], J. Nystrand[13], F.E. Obenshain[20], A. Oskarsson[13], I. Otterlund[13], M. Pachr[15], A. Parfenov[6], S. Pavliouk[6], T. Peitzmann[9], V. Petracek[15], F. Plasil[7], W. Pinganaud[10], M.L. Purschke[11], B. Raeven[12], J. Rak[15], R. Raniwala[2], S. Raniwala[2], V.S. Ramamurthy[19], N.K. Rao[8], F. Retiere[10], K. Reygers[9], G. Roland[18], L. Rosselet[4], I. Roufanov[6], C. Roy[10], J.M. Rubio[4], H. Sako[14], S.S. Sambyal[8], R. Santo[9], S. Sato[14], H. Schlagheck[9], H.-R. Schmidt[11], Y. Schutz[10], G. Shabratova[6], T.H. Shah[8], I. Sibiriak[5], T. Siemiarczuk[17], D. Silvermyr[13], B.C. Sinha[3], N. Slavine[6], K. Söderström[13], N. Solomey[4], S.P. Sørensen[7,20], P. Stankus[7], G. Stefanek[17], P. Steinberg[18], E. Stenlund[13], D. Stüken[9], M. Sumbera[15], T. Svensson[13], M.D. Trivedi[3], A. Tsvetkov[5], L. Tykarski[17], J. Urbahn[11], E.C.v.d. Pijll[12], N.v. Eijndhoven[12], G.J.v. Nieuwenhuizen[18], A. Vinogradov[5], Y.P. Viyogi[3], A. Vodopianov[6], S. Vörös[4], B. Wysłouch[18], K. Yagi[14], Y. Yokota[14], G.R. Young[7]

[1] University of Panjab, Chandigarh 160014, India
[2] University of Rajasthan, Jaipur 302004, Rajasthan, India
[3] Variable Energy Cyclotron Centre, Calcutta 700 064, India
[4] University of Geneva, 1211 Geneva 4, Switzerland
[5] RRC "Kurchatov Institute", 123182 Moscow, Russia
[6] Joint Institute for Nuclear Research, 141980 Dubna, Russia
[7] Oak Ridge National Laboratory, Oak Ridge, TN 37831-6372, USA
[8] University of Jammu, Jammu 180001, India
[9] University of Münster, 48149 Münster, Germany
[10] SUBATECH, Ecole des Mines, Nantes, France
[11] Gesellschaft für Schwerionenforschung (GSI), 64220 Darmstadt, Germany
[12] Universiteit Utrecht/NIKHEF, 3508 TA Utrecht, The Netherlands
[13] Lund University, 221 00 Lund, Sweden
[14] University of Tsukuba, Ibaraki 305, Japan
[15] Nuclear Physics Institute, 250 68 Rez, Czech Rep.
[16] KVI, University of Groningen, 9747 AA Groningen, The Netherlands
[17] Institute for Nuclear Studies, 00-681 Warsaw, Poland
[18] MIT Cambridge, MA 02139, USA
[19] Institute of Physics, 751-005 Bhubaneswar, India
[20] University of Tennessee, Knoxville, TN 37966, USA

Abstract. Transverse energy, charged particle pseudorapidity distributions and photon transverse momentum spectra have been studied as a function of the number of participants (N_{part}) and the number of binary nucleon-nucleon collisions (N_{coll}) in 158·A GeV Pb+Pb collisions over a wide impact parameter range. A scaling of the transverse energy pseudorapidity density at midrapidity as $\sim N_{part}^{1.08\pm0.06}$ and $\sim N_{coll}^{0.83\pm0.05}$ is observed. For the charged particle pseudorapidity density at midrapidity we find a scaling as $\sim N_{part}^{1.07\pm0.04}$ and $\sim N_{coll}^{0.82\pm0.03}$. This faster than linear scaling with N_{part} indicates a violation of the naive Wounded Nucleon Model.

1 Introduction

Heavy-ion collisions at ultrarelativistic energies probe nuclear matter at high temperatures and densities. A major goal of these studies is the search for a deconfined phase of nuclear matter. A necessary condition to reach such a phase transition is local equilibration as might be achievable through rescattering of the produced particles. Since the amount of rescattering should increase with the size of the reaction system, it is of interest to study these reactions over a wide range of centralities.

For hard processes, where cross sections are small, the naive expectation is a scaling of the particle yields with the number of binary collisions. Experimentally, the scaling of cross sections with target mass in p+A collisions was studied and the scaling was observed to be even stronger than this expectation [1]. This was later attributed to multiple parton scattering in the initial state [2,3]. From the same experiment it was also seen that particle production at intermediate p_T shows a much weaker increase with target mass.

The gross features of particle production in nucleon-nucleus collisions and reactions of light nuclei are well described in the framework of the Wounded Nucleon Model [4]. In this model the transverse energy and particle production in p+A and A+A reactions is calculated by assuming a constant contribution from each participating nucleon. This kind of scaling has also been observed by the WA80 collaboration in reactions of ^{16}O and ^{32}S projectiles with various targets where $dE_T/d\eta|_{max}$ was found to depend approximately linearly on the average total number of participants [5].

While a scaling with the number of collisions arises naturally in a picture of a superposition of nucleon-nucleon collisions, with a possible modification by initial state effects, the Wounded Nucleon Model or participant scaling is more naturally related to a system with strong final state rescattering, where the incoming particles lose their memory and every participant contributes a similar amount of energy to particle production. The scaling behavior of particle production may therefore carry important information on the reaction dynamics. Various experimental signatures in heavy ion reactions require a comparison of observables for different system sizes. Therefore it is important to have a good understanding of these basic scaling properties. The scaling behavior can also be used as a valuable test for models of particle production in heavy ion reactions (see e.g. [6]).

Furthermore, several observables in heavy ion reactions seem to show qualitative changes once a certain system size is reached. Strangeness production is enhanced in S+S reactions compared to p+p, but seems to saturate for even larger nuclei (see e.g. [7]). Recent results from the WA98 experiment [8] show a significant change of the shape of the π^0 p_T spectrum in peripheral Pb+Pb collisions compared to p+p data. The shape, however, remains unchanged in the range of semi-central Pb+Pb collisions with about 50 participating nucleons up to central reactions.

The NA50 collaboration has observed an anomalously suppressed J/ψ yield in central Pb+Pb collisions in contrast to peripheral reactions [10] where the suppression of the J/ψ yield can be explained by absorption in nuclear matter. This anomalous J/ψ suppression provides an additional incentive to study the scaling behavior of particle production with the number of participants. Most models based on J/ψ absorption by hadronic comovers assume the comover density to scale linearly with the number of participants and are then not able to fit the anomalous suppression [11,12]. Only if the hadronic comover density scales substantially faster than linearly with the number of participants it is possible to obtain reasonable fits to the anomalous suppression. It is therefore of interest to study in detail the centrality dependence of particle production and investigate its scaling properties with respect to the number of participants or collisions.

2 Experiment and data analysis

The CERN experiment WA98 is a general-purpose apparatus which consists of large acceptance photon and hadron spectrometers together with several other large acceptance devices which allow to measure various global variables on an event-by-event basis. The experiment took data with the 158·A GeV ^{208}Pb beams from the CERN SPS in 1994, 1995, and 1996. The layout of the WA98 experiment as it existed during the final WA98 run period in 1996 is shown in Fig. 1. The data presented here were taken during the 1996 lead beamtime. The transverse energy and charged particle distributions shown in this paper were measured with the magnetic field of the Goliath magnet turned off. The minimum bias cross section for this configuration was $\sigma_{mb} = (6260 \pm 280)$ mb. The error of the minimum bias cross section relates to the uncertainty of the target thickness and the uncertainty in the subtraction of the contribution from interactions outside the target. The contribution of these interactions was determined in special target-out runs. A 20% uncertainty of this contribution was assumed in the calculation of the uncertainty of the minimum bias cross section. The WA98 experiment took most of the data with the Goliath
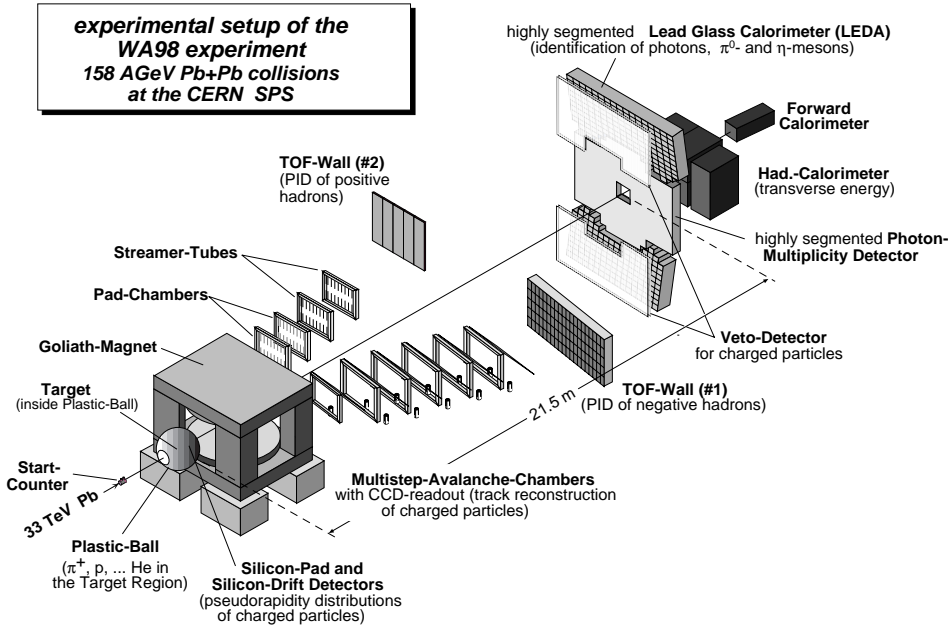
Fig. 1. The WA98 experimental setup

magnet turned on. Since the analysis of the photon and neutral pion scaling requires high statistics the respective spectra used here were measured in a field-on configuration. The minimum bias cross section for this data set was $\sigma_{mb} = (6440 \pm 300)$ mb.

The Zero Degree Calorimeter is located 30 m downstream of the target and measures the total energy of all particles within an angle $\Theta < 0.3°$ relative to the beam axis in the laboratory system. The MIRAC calorimeter is placed 24 m downstream of the target [13]. It consists of a hadronic and an electromagnetic section and covers the pseudorapidity interval $3.5 < \eta < 5.5$. MIRAC plays the central role in the WA98 minimum bias trigger where the measured E_T is required to be above a minimum threshold. The systematic errors of $dE_T/d\eta$ at midrapidity are dominated by the correction for the differences in the response of the MIRAC to hadronic and electromagnetic showers and to the extrapolation of the distribution of $dE_T/d\eta$ to midrapidity. These combine to give an overall systematic uncertainty of $\approx 20\%$ in the absolute result for $dE_T/d\eta|_{max}$. The centrality dependent part of this uncertainty is much smaller and estimated to be approximately 5% only. The correction of $dE_T/d\eta$ due to interactions outside the target for peripheral Pb+Pb reactions is less than 2%.

The charged particle multiplicity is measured with a circular Silicon Pad Multiplicity Detector (SPMD) located 32.8 cm downstream of the target [14]. It consists of four quadrants each produced from a 300 μm thick silicon wafer. This detector provides full azimuthal coverage of the pseudorapidity region $2.35 < \eta < 3.75$ with 180 Φ-bins and 22 η-bins. The pad size increases radially to provide an approximately uniform pseudorapidity coverage. In central Pb+Pb collisions the probability that a pad is hit by two or more particles is not negligible. Therefore the multiplicity in an η-ring is determined from the sum of the measured energy losses of the charged parti-

cles traversing the η-ring divided by the average energy loss per charged particle. The charged particle pseudorapidity distribution is corrected for δ-electrons produced by lead ions traversing the 213 μm thick ^{208}Pb target foil. On average these electrons give rise to roughly 11 additional hits in the SPMD. This contribution has been determined from beam triggers where no inelastic interaction took place. The systematic error of $dN_{ch}/d\eta$ relates to the uncertainty in the determination of the total energy loss of the charged particles in the SPMD and to the correction for δ-electrons. The uncertainty in the energy loss measurement is estimated to result in a 3% centrality independent systematic error. The correction for δ-electrons at midrapidity $(dN_\delta/d\eta|_{mid} \approx 9)$ is assumed to be known with an accuracy of 10% and contributes significantly to the total uncertainty only for peripheral reactions. However, the $dN_{ch}/d\eta$ distributions as shown in Fig. 6 exhibit a slight asymmetry around midrapidity. We can force the $dN_{ch}/d\eta$ distribution to be symmetric by arbitrarily increasing the subtracted δ-electron contribution. For central events the δ-electron yield has to be increased by roughly 80%. This factor decreases when going to semi-central and peripheral events. It's difficult to imagine a physical reason for a much larger δ-electron production than what was measured for beam triggers. However, by making these extreme assumptions we estimate the centrality dependent error of $dN_{ch}/d\eta$ by comparing the $dN_{ch}/d\eta$ distributions with δ-electrons subtracted as measured in beam events with the $dN_{ch}/d\eta$ distributions that were forced to be symmetric. For peripheral and semi-central events this uncertainty typically is of the order of $3 - 4\%$ and decreases to 2% in central events. The correction of $dN_{ch}/d\eta$ measured with the SPMD in peripheral events due to interactions outside the target is typically of the order of 15%. The uncertainty of $dN_{ch}/d\eta$ due to this correction is estimated to be around 3%.

The photon distributions used in this analysis were measured with the LEDA spectrometer in the rapidity interval $2.3 < \eta < 3.0$. This detector is located 21.5 m from the target and consists of 10080 leadglass modules each read out by a photomultiplier. A streamer tube array placed directly in front of LEDA was used as a charged particle veto detector to correct for the charged hadron contamination in the leadglass. The remaining correction for neutrons and anti-neutrons has been made based on simulation results using the GEANT package [15]. The detection efficiency of photons in LEDA is based on GEANT simulations and experimental data in order to take into account the effects of overlapping showers which can result in a shift in the measured transverse momentum. These corrections require high statistics and therefore only 8 centrality classes have been used for the photon analysis here. These are the same 8 centrality classes used in the analysis of the scaling of neutral pion production presented in [8]. The systematic error on the photon and neutral pion multiplicities is estimated to be $\approx 10\%$ mainly originating from corrections for efficiency and contamination.

3 Model calculations

In the present analysis, the photon and charged particle scaling has been investigated with the centrality of the Pb+Pb collision determined from the transverse energy, E_T, measured with the MIRAC calorimeter. However, in the E_T scaling analysis, the forward energy E_F of projectile spectators measured with the Zero Degree Calorimeter has been used for the centrality selection, in order to avoid auto-correlations. Twenty-one centrality classes have been defined based on the measured E_T. Each class corresponds to 5% of the minimum bias cross section, with an additional very central class corresponding to the 1% most central events. The ZDC cannot resolve the centrality of very peripheral collisions as well as the MIRAC calorimeter and therefore the E_T scaling analysis is limited to centrality classes which correspond to more than approximately 40 participants.

The number of participants N_{part} and collisions N_{coll} for a given centrality class have been determined from a simulation based on the event generator VENUS 4.12 [16]. Control calculations were made with the FRITIOF event generator [29]. The definition of N_{part} and N_{coll} in these models is based on a geometrical picture (Glauber model) where nucleons travel on straight-line trajectories and the nucleon-nucleon cross section is independent of the number of collisions a nucleon has undergone before. The approach of using event generators allowed to take into account the energy resolution of the ZDC and MIRAC calorimeters. Furthermore, the minimum bias trigger efficiency has been included in the simulation. Figure 2 shows a comparison of the measured E_T and E_F distributions to the VENUS simulations. The overall agreement in the E_T distribution between the data and the model is good. However, the VENUS prediction extends to slightly higher transverse energy for the most central reactions. In the
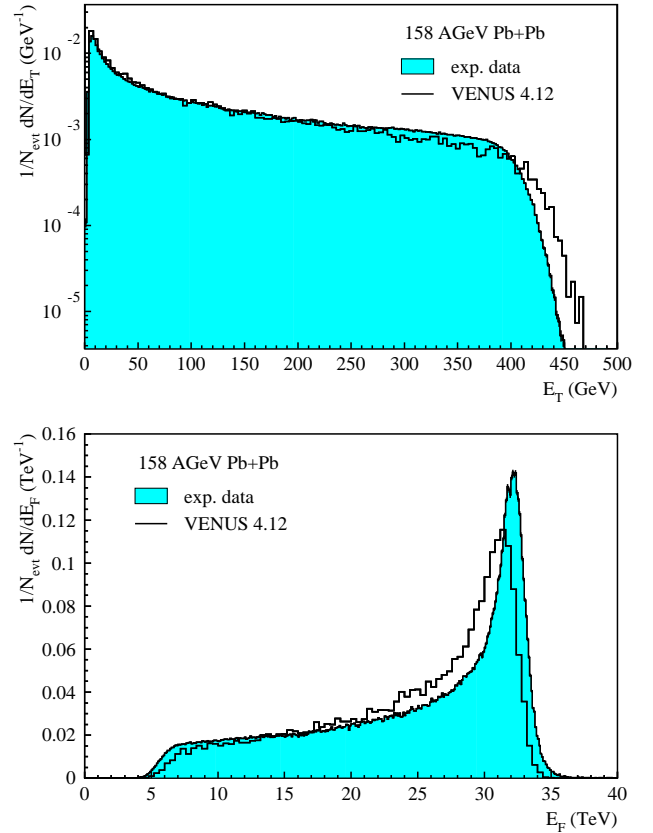

Fig. 2. Distributions of the transverse energy E_T as measured in MIRAC (upper graph) and the forward energy E_F as measured with the ZDC (lower graph) in 158·A GeV Pb+Pb collisions. Predictions of the event generator VENUS 4.12 are included

forward energy distribution, the strong peak for peripheral reactions is not precisely reproduced, while the general shape is quite similar. Also the event-by-event anti-correlation of E_T and E_F observed in the experimental data is in good agreement with the model calculations (see Fig. 3).

To obtain a robust estimate of N_{part} and N_{coll}, which is less sensitive to discrepancies in the energy distributions, the centrality classes in the model have been chosen to represent the same absolute cross section as the data. The effect of the centrality cuts on the distributions of the number of participants can be seen from Fig. 4, where distributions of N_{part} for centrality classes corresponding to fractions of the minimum bias cross section of 0-1%, 1-5%, 5-10%, 10-20%, 20-40%, 40-60%, 60-80% and 80-100% are shown. One can see that the limited acceptance, the detector resolution, and the fluctuations in particle production as implemented in the model lead to an overlap of the distributions of adjacent centrality classes. Nevertheless, it is observed that even a strong cut on the 1% most central reactions yields a significantly different selection than e.g. the 5% most central reactions.

Figure 5 shows a summary of the RMS-values versus the average values of the distributions of N_{part} for the centrality selections as used in the later analysis in this
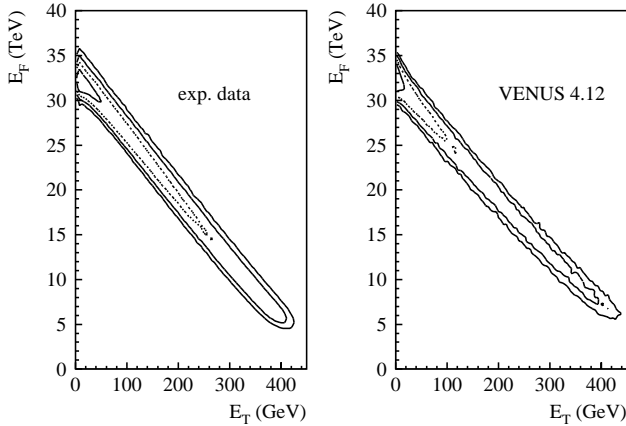
Fig. 3. Event-by-event distributions of the transverse energy E_T vs. the forward energy E_F in 158·A GeV Pb+Pb collisions. The left plot shows the experimental data and the right plot predictions of the event generator VENUS 4.12
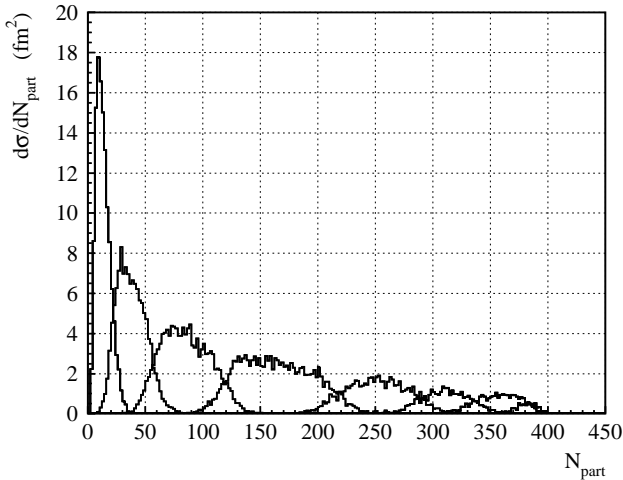

Fig. 4. Distributions of the number of participants N_{part} obtained from VENUS 4.12 for different centrality classes selected by the transverse energy E_T
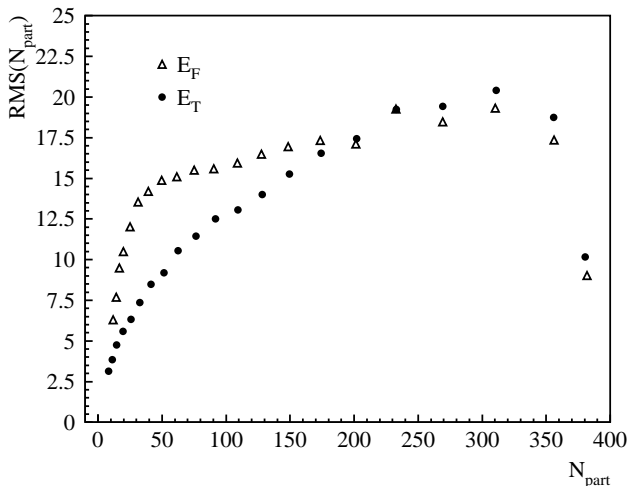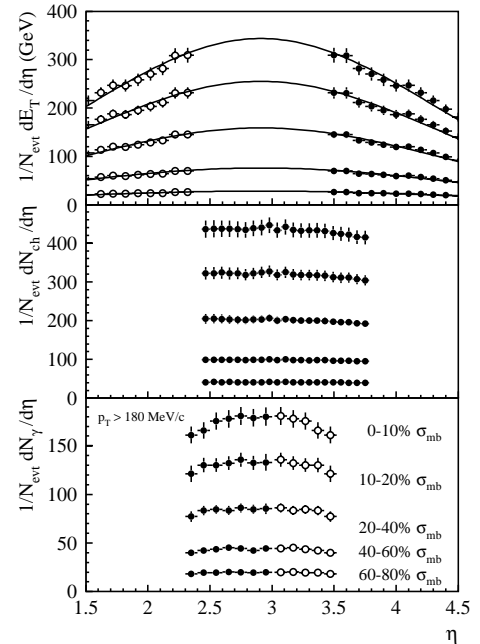

Fig. 5. RMS-values of the number of participants N_{part} obtained from VENUS 4.12 for different centrality classes selected by the transverse energy E_T and the forward energy E_F

Fig. 6. Pseudorapidity distributions of transverse energy, charged particles and photons measured in 158·A GeV Pb+Pb collisions of different centrality. Photons were measured above a lower transverse momentum threshold of 180 MeV/c. The open symbols have been obtained by reflecting the measured data points at midrapidity

paper. While the classes selected with E_F have a slightly smaller width for very central reactions, for peripheral reactions the resolution of the selection is much better using E_T.

The precise number of participants or number of collisions may, however, depend on the specific model assumptions. We have therefore performed a detailed study of the influence of these assumptions and other sources of systematic errors for the analysis presented here. A summary of these studies is given in Appendix A.

4 Results

The pseudorapidity distributions for the transverse energy, the charged particle multiplicity, and the photon multiplicity are shown in Fig. 6 for five centrality classes. All distributions have been corrected for possible contributions of reactions upstream and downstream of the target and in the target frame by subtracting the respective yield determined in target-out runs, see [19] for further details. To obtain $dE_T/d\eta|_{max}$ the measured data points have been reflected at midrapidity ($\eta_{cm} = 2.91$) and fitted with a Gaussian.

A first impression of the centrality dependence of E_T and charged particle production can be obtained by normalizing the yields to the number of participants. This is shown in Fig. 7. Both for E_T and the charged multiplicity the yield per participant increases when going from peripheral to more central reactions. As described in the
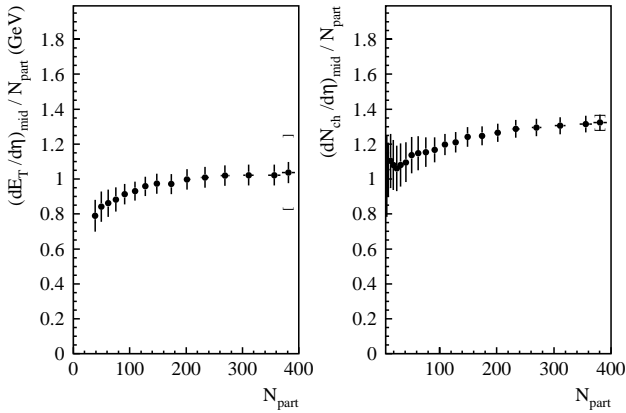
Fig. 7. Transverse energy and charged particle yields in 158·A GeV Pb+Pb reactions normalized to the number of participants as a function of the number of participants. For the number of participants an uncertainty as indicated in Fig. 16 was assumed. Furthermore, all centrality dependent errors of $dE_T/d\eta$ and $dN_{ch}/d\eta$ as described in Sect. 2 were taken into account in the calculation of the error bars. The brackets indicate the centrality independent uncertainty of the overall $dE_T/d\eta$ and $dN_{ch}/d\eta$ scale
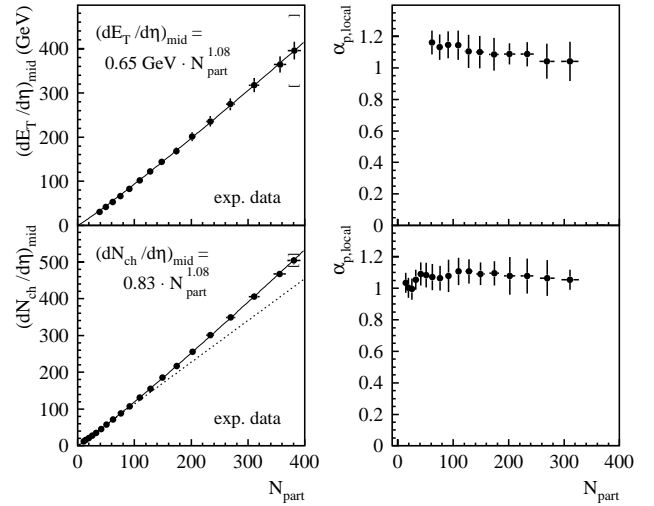

Fig. 8. Pseudorapidity density of E_T and N_{ch} at midrapidity as a function of the number of participants. The participant numbers shown here were calculated in a VENUS simulation (denoted as calculation A in the appendix). Both for E_T and N_{ch} the fit results obtained from a fit of all data points are shown. In order to demonstrate the stronger than linear increase of the data points a linear extrapolation of the charged particle multiplicity in peripheral Pb+Pb reactions ($N_{part} \approx 50$) is shown as a dotted line in the lower left plot. The scaling behavior can be verified in more detail on the right panel where the local scaling exponents are shown. The local scaling exponents have been obtained from a fit of 5 neighboring E_T and N_{ch} data points

appendix we have also used the FRITIOF model instead of VENUS to calculate the number of participants and the number of nucleon-nucleon collisions. The results of these two calculations for the number of participants are compared in the appendix (Fig. 16) and used to obtain the estimated uncertainty of the number of participants which was used in the calculation of the error bars in Fig. 7.

The scaling behavior is studied in more detail in Fig. 8 which shows the dependence of the E_T and N_{ch} pseudorapidity densities at midrapidity on the number of participants. The scaling behavior of these observables was parameterized as

$$\left.\frac{dX}{d\eta}\right|_{mid} \sim N_{part}^{\alpha_p},\ N_{coll}^{\alpha_c}, \quad X = E_T,\ N_{ch}. \qquad (1)$$

This functional dependence gives a reasonable description of the data for the entire centrality range. Taking the number of participants from the VENUS calculation (denoted as calculation A in the appendix) the charged particle scaling can be described by a scaling exponent $\alpha_p = 1.08$. The calculations of the number of participants using VENUS, or VENUS with an experimentally determined nucleon density distribution, or FRITIOF (denoted as calculations A, B, and F in the appendix) are all based on reasonable assumptions. These three calculations give slightly different participant numbers. We quote the average of the corresponding three scaling exponents α_p as the final result. As described in the appendix the estimated uncertainty of α_p due to the uncertainty of the number of participants is 0.036. In the fit from which we obtain the value of α_p we only take the statistical error of the data points into account. Since the statistical errors are small the fit error is negligible. In order to estimate the influence of the centrality dependent errors of $dN_{ch}/d\eta$ on α_p we systematically move the data points within the error

bars and repeat the fit. From this procedure we estimate an uncertainty of 0.02 for α_p due to the centrality dependent errors of $dN_{ch}/d\eta$. Adding all errors in quadrature we finally obtain $\alpha_p = 1.07 \pm 0.04$ for the charged particle scaling.

For the E_T scaling we perform a similar error analysis. An additional uncertainty comes from the assumed centroid of the $dE_T/d\eta$ distribution. Primarily due to massive particles like protons and neutrons, the difference between pseudorapidity and rapidity could lead to an increase of the centroid relative to midrapidity ($y_{mid} = 2.91$). By varying the assumed $dE_T/d\eta$ centroid position in the η-range 2.91 ± 0.3 a corresponding error of 0.02 was estimated for the E_T scaling exponent α_p. Adding all errors in quadrature we obtain $\alpha_p = 1.08 \pm 0.06$.

In more detail, the relative scaling for different centralities can be judged from the *local scaling exponent* α_{local} shown on the right hand side of Fig. 8. These have been obtained from a fit of 5 neighboring E_T and N_{ch} data points. For the charged particles it can be seen that the scaling remains approximately constant over the whole centrality range. For E_T the local scaling exponent appears to be almost constant in the range $N_{part} > 100$. However, below $N_{part} \approx 100$ the local scaling exponent seems to increase slightly.

Considering the scaling with the number of binary nucleon-nucleon collisions and averaging the results determined with calculations A, B, and F we obtain a similarly
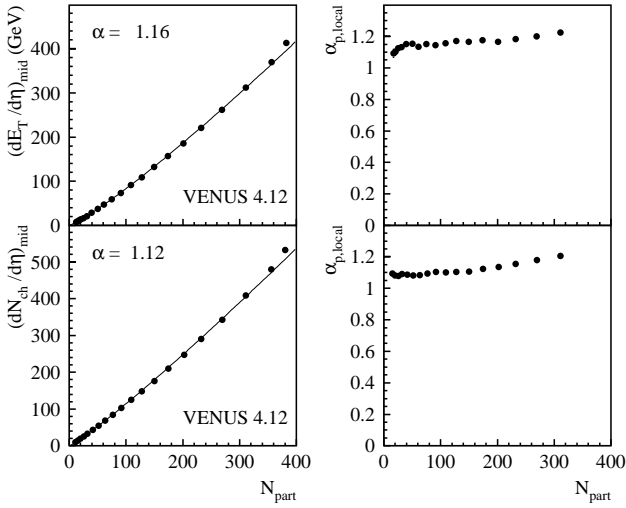
Fig. 9. Pseudorapidity density of E_T and N_{ch} at midrapidity as a function of the number of participants as in Fig. 8 from VENUS 4.12 simulations

Fig. 10. Pseudorapidity density of N_{ch} at midrapidity as a function of the number of participants for p+p [22] and Pb+Pb collisions. The number of participants shown here were calculated using VENUS (calculation A in the appendix). The fit function plotted as a solid line is the same as obtained in Fig. 8. The dashed function is the fit result using the participant values from the FRITIOF calculation (calculation F). On the right hand side the ratio of the data (using participants from VENUS) to the fit function is shown

good description with $\alpha_c = 0.82\pm0.03$ for the charged particle scaling. For the E_T scaling we obtain $\alpha_c = 0.83\pm0.05$. These results are not surprising since for symmetric systems one naively expects a scaling relation to hold between the number of collisions and the number of participants:

$$N_{coll} \propto N_{part}^{\alpha_{cp}} \text{ with } \alpha_{cp} = \frac{4}{3}. \qquad (2)$$

Fits of the parameters extracted from VENUS simulations indeed yield a value of $\alpha_{cp} = 1.28$ which is close to the above value. For a scaling with $N_{part}^{1.08}$ this would lead to a behavior as $N_{coll}^{0.84}$.

A similar analysis can be performed on the data obtained from the VENUS simulation itself. The results of such an analysis are displayed in Fig. 9. It is observed that the scaling exponents are higher in the simulation, and that both for E_T and N_{ch} the exponent α shows a tendency to increase with centrality. We note here that the extraction of the number of participants and the number of binary nucleon-nucleon collisions is almost completely independent of the scaling exponent present in the underlying event generator. As described in Sect. 3 this is due to the fact that the centrality classes defined in the model calculations correspond to the same absolute cross section as the experimental centrality classes.

It is interesting to extrapolate this scaling towards smaller system sizes and compare to the expectation from pp collisions [22]. This has been done in Fig. 10. It can be seen that the scaling obtained from charged particle production in Pb+Pb collisions extrapolates nicely to pp collisions. In particular, there is no threshold effect visible in the charged particle multiplicity when going to central Pb+Pb collisions.

In a recent publication [18] we have discussed the systematics of inclusive photon production as measured with the WA98 Photon Multiplicity Detector. There it was found that the pseudorapidity density of photons at midrapidity scales with the number of participants as
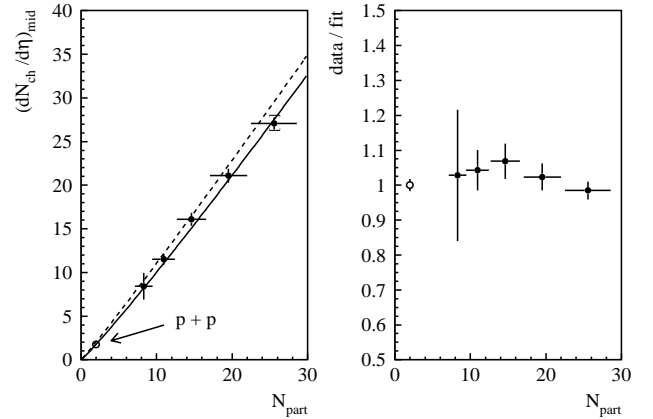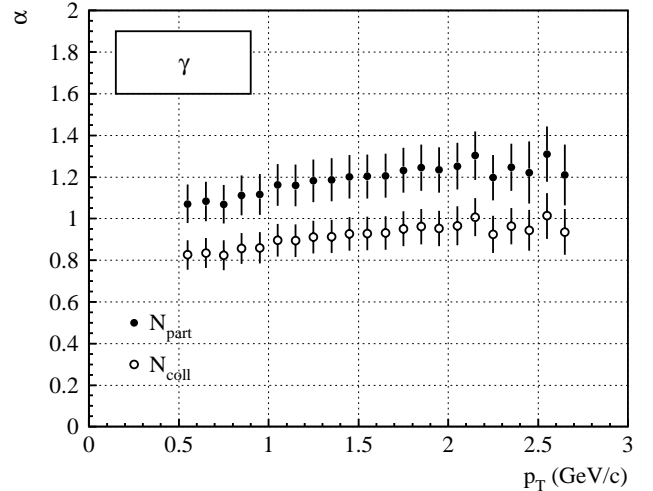

Fig. 11. Exponents for a scaling with the number of participants and nucleon-nucleon collisions for photons measured in LEDA as a function of the transverse momentum. Only reactions with $N_{part} \geq 30$ have been used. The data points shown were obtained using the number of participants from VENUS. The error bars reflect the uncertainty of the photon measurement, the uncertainty in the calculation of N_{part}/N_{coll} and the fit error

$N_{part}^{1.12\pm0.03}$. This is slightly larger, but consistent with the exponent from the present analysis of E_T and N_{ch}. Photon production can be investigated in further detail with the photon spectrometer LEDA. It can very naturally be studied as a function of the transverse momentum. The corresponding scaling exponents α extracted are shown in Fig. 11. The photon measurement in LEDA suffers from larger systematic uncertainties at low momenta, so only photons for $p_T > 500$ MeV/c have been considered. At

a transverse momentum of $p_T \approx 500$ MeV/c the inclusive photon yield shows a scaling behavior similar to that observed for E_T and N_{ch}. However, the extracted scaling exponents tend to rise with increasing p_T and at $p_T \approx 2$ GeV/c the scaling can be described as $\sim N_{part}^{1.2}$ and $\sim N_{coll}^{0.9}$.

Since a large fraction of the inclusive photons originates from the decay of neutral pions it is of interest to compare the scaling of photons to that of neutral pions which have already been discussed in [8]. These data have been reanalyzed [9] and the results of the scaling exponents with respect to the number of participants are shown in Fig. 12. The values are nearly constant at $\alpha \approx 1.1$ with a tendency to decrease towards higher transverse momenta. It should be noted that the extracted exponents are smaller compared to the values given in [8]. This is mostly due to a more sophisticated calculation of the number of participants used here.

We have recently published results on the production of direct photons in 158·A GeV Pb+Pb collisions [20, 21]. A significant yield of direct photons at $p_T > 1.5$ GeV/c is observed in central collisions, while in peripheral collisions the photon production is consistent with the yield expected from the decays of neutral pions, η mesons, and other hadrons. At $p_T \approx 2$ GeV/c the direct photon yield in central collisions amounts to roughly 20% of the photons from hadronic decays. The scaling of the neutral pion yield presented in Fig. 12 appears to be consistent with the scaling of charged particles and the transverse energy, while the photon yield at higher transverse momenta seems to increase more strongly with the number of participants. We assume that for a relatively small yield of direct photons in central collisions, the centrality dependence of the inclusive photons can still be described with a scaling law as in (1). It's then obvious that the production of direct photons in central Pb+Pb collisions necessarily increases the scaling exponent α of the inclusive photons at high transverse momenta. In this respect the behavior of the extracted scaling exponents for inclusive photon and neutral pion production are consistent with the direct photon excess observed in central Pb+Pb collisions. However, due to the uncertainties of the scaling exponents for photons and neutral pions it is not possible to draw quantitative conclusions about direct photon production from Figs. 11 and 12.

In simple multiple collision models a heavy ion reaction is regarded as a sequence of independent nucleon-nucleon collisions which can be described as in free space [23, 24]. After a projectile nucleon suffers an inelastic collision the assumption of local baryon number conservation assures that a baryon-like object is still present. This baryon-like object is assumed to contribute to the particle production in subsequent collisions with the same cross section as the initial nucleon. In this picture the contribution of each nucleon-nucleon collision is added incoherently which leads to a linear scaling of E_T and particle production with the number of binary collisions. If the energy degradation in each nucleon-nucleon reaction is taken into account a reasonable description of E_T and particle production can
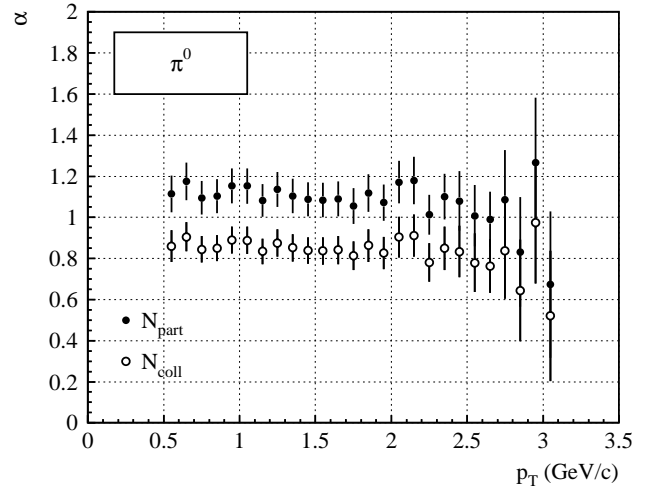

Fig. 12. Exponents for a scaling with the number of participants and nucleon-nucleon collisions for neutral pions measured in LEDA as a function of the transverse momentum. Only reactions with $N_{part} \geq 30$ have been used. The data points shown were obtained using the number of participants from VENUS. The error bars reflect the uncertainty of the π^0 measurement, the uncertainty in the calculation of N_{part}/N_{coll} and the fit error

be obtained. The approximate scaling as $N_{coll}^{0.83}$ for the transverse energy and charged particles may be used to obtain information on the average energy degradation in a nucleon-nucleon collision.

A simple way of investigating this hypothesis is to study the particle production per binary collision as a function of the effective thickness x of the two nuclei, which might be characterized in the following way [23–25]:

$$\frac{dN_{ch}}{d\eta}(AA) = N_{coll} \cdot f(x) \cdot \frac{dN_{ch}}{d\eta}(pp). \qquad (3)$$

Here $f(x)$ should describe the effect of energy degradation on particle production with x being a suitable thickness variable – we have chosen $x \equiv N_{coll}/N_{part}$. Figure 13 shows the pseudorapidity density of N_{ch} at midrapidity in Pb+Pb collisions normalized to the number of collisions and the charged particle density in pp collisions. The data show a continuous decrease of the multiplicity per collision for increasing x, i.e. the more collisions a participant suffers, the smaller is the contribution of each collision to particle production. As an example, this can be illustrated more quantitatively for the centrality classes with $N_{coll}/N_{part} \approx 1$, i.e. for the case that each participating nucleon on the average suffers two nucleon-nucleon collisions. For these reactions the actual charged particle density at midrapidity is 40% lower than one would expect from a linear scaling of the charged particle density in pp reactions with the number of binary nucleon-nucleon collisions. In a simple multiple collision picture this means that on the average the second collisions of each participant contributes only 20% of the yield of the first collision to the charged multiplicity at midrapidity.
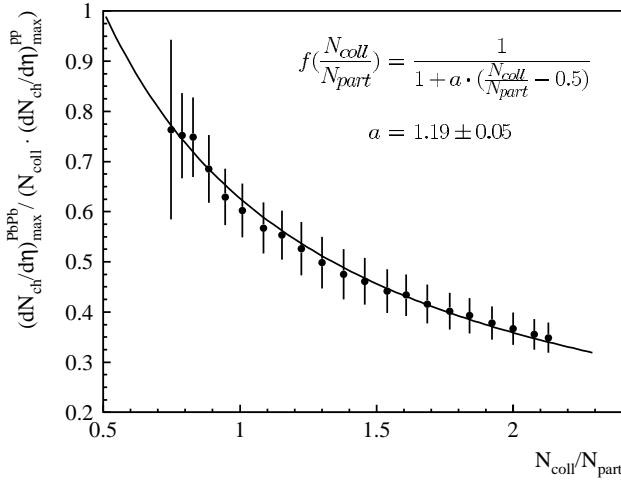
Fig. 13. Pseudorapidity density of N_{ch} at midrapidity in Pb+Pb collisions normalized to the number of collisions and the charged particle density in pp collisions. The solid line shows a fit with (4)
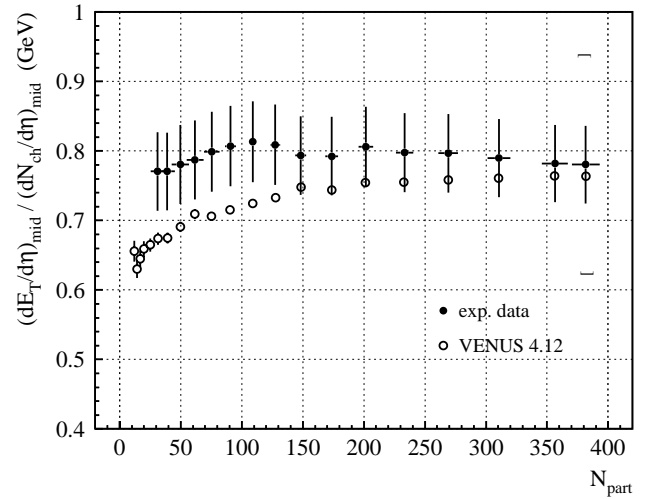

Fig. 14. $\langle E_T \rangle / \langle N_{ch} \rangle|_{mid}$ as a function of the number of participants. For comparison results of VENUS 4.12 calculations are included. The error bars indicate the centrality dependent errors of the experimental result. The overall uncertainty of $\langle E_T \rangle / \langle N_{ch} \rangle|_{mid}$ which is mainly due to the uncertainty in $(dE_T/d\eta)_{mid}$ is indicated by brackets

In proton-nucleus reactions multiplication of the charged particle multiplicity observed in pp reactions by the number of binary nucleon-nucleon collisions overestimates the measured multiplicity by $20-30\%$ [26, 27]. In case of proton-nucleus reactions the target participants suffer exactly one nucleon-nucleon collision. This is of course not true in AA collisions. Nevertheless, it is interesting to apply the same recipe to heavy ion reactions. Figure 13 shows that multiplying the pp yield with the number of binary nucleon-nucleon collisions gives as much as 60% too many charged particles in central Pb+Pb reactions.

We have attempted to fit the data in Fig. 13 with the form:

$$ f_{fit}\left(\frac{N_{coll}}{N_{part}}\right) = \left[1 + a\left(\frac{N_{coll}}{N_{part}} - 0.5\right)\right]^{-1}. \quad (4) $$

This function basically represents a first order Taylor approximation of the function $1/f$ in (3). A good fit is obtained with $a = 1.19 \pm 0.05$.

In the case of the Wounded Nucleon Model the eventual fragmentation of an excited nucleon after an inelastic collision is not affected by further collisions with other nucleons, no matter how many times it is successively struck. The observation of a stronger than linear increase of E_T and N_{ch} with the number of participants indicates that this model is only approximately correct. It can be clearly seen, regarding the two possible centrality variables investigated here, that the number of participants is better suited, because the scaling exponent is closer to one compared to the number of collisions.

With the present data it is possible to determine the average transverse energy per charged particle at midrapidity

$$ \langle E_T \rangle / \langle N_{ch} \rangle|_{mid} \equiv \langle dE_T/d\eta|_{mid} \rangle / \langle dN_{ch}/d\eta|_{mid} \rangle, \quad (5) $$

a quantity that can be seen as a measure of the global mean transverse momentum averaged over all particle species. $\langle E_T \rangle / \langle N_{ch} \rangle|_{mid}$ is plotted in Fig. 14 as a function of centrality, represented by the number of participants. For this figure both $dE_T/d\eta$ and $dN_{ch}/d\eta$ were evaluated in identical centrality classes, defined with the forward energy E_F.

$\langle E_T \rangle / \langle N_{ch} \rangle|_{mid}$ appears to increase up to a system size of $N_{part} \approx 100$ which corresponds to an impact parameter of $b \approx 9$ fm. For more central collisions $\langle E_T \rangle / \langle N_{ch} \rangle|_{mid}$ levels off at a value of 0.80 GeV. This value is slightly higher than the maximum $\langle E_T \rangle / \langle N_{ch} \rangle|_{mid} \approx 0.66$ GeV observed in 200·A GeV S+Au and S+Al reactions [17]. VENUS 4.12 predicts a qualitatively similar behavior for $\langle E_T \rangle / \langle N_{ch} \rangle|_{mid}$, while the absolute value is approximately 100 MeV lower at $N_{part} \approx 100$. One may also note that the VENUS results continue to rise by ≈ 50 MeV when going from $N_{part} \approx 100$ to $N_{part} \approx 400$, while the experimental data appear to be completely flat in this region. A similar saturation with increasing number of participants as observed here has been seen in the (truncated) mean p_T of neutral pions with $p_T > 400$ MeV/c produced in Pb+Pb reactions [8]. A natural explanation of such a behavior would be the assumption that thermalization is reached once the system exceeds a certain minimum size.

5 Conclusions

We have analyzed the dependence of transverse energy and charged particle pseudorapidity distributions and photon transverse momentum spectra in 158·A GeV Pb+Pb collisions on the number of participants and the number of binary nucleon-nucleon collisions. A scaling behavior as $N_{part}^{1.07\pm0.04}$ and $N_{coll}^{0.82\pm0.03}$ describes the

charged particle production over the whole impact parameter range. The E_T production was studied for collisions with more than approximately 40 participants. In this centrality range the E_T production scales as $N_{part}^{1.08\pm0.06}$ and $N_{coll}^{0.83\pm0.05}$.

Photons at $p_T \approx 500$ MeV/c show a scaling behavior similar to the scaling of E_T and N_{ch}. The p_T-dependence of the photon scaling was studied and a rise of the extracted scaling exponents with increasing transverse momentum was found.

We have studied the transverse energy per charged particle as a function of centrality and found an indication of an increase from peripheral to semi-central collisions with approximately 100 participants with a subsequent saturation for larger systems.

While the global variables like E_T and charged particle multiplicity seem to scale closer to the number of participants than to the number of binary collisions, there is a clear participant scaling violation compared to a purely linear dependence. This scaling violation might e.g. have consequences for the suppression of J/ψ production from comovers, since the implied central particle densities are considerably larger than estimated based on a linear scaling.

Appendix A: Systematic uncertainties in model calculations

In order to obtain an estimate of the systematic uncertainties in the calculation of the number of participants and the number of nucleon-nucleon collisions we have varied several assumptions in the model calculations. The dependence of the particle and transverse energy yield on the number of participants and collisions is described with the scaling exponents α_p and α_c in this paper. In this section we investigate how the extracted scaling exponents α_p and α_c for the charged particle yield (with similar conclusions for the other observables) are affected by the different model assumptions.

In the VENUS 4.12 simulations used to obtain the number of participants and collisions we have varied

- the parameterization of the nucleon density distribution,
- the energy resolution of MIRAC and
- the minimum bias cross section.

As a cross check we have also calculated the number of participants and collisions using the event generator FRITIOF [29].

The nuclear density profile used in VENUS and FRITIOF is an effective parameterization using a Woods-Saxon shape:

$$\rho(r) = \rho_0 \cdot \frac{1}{1 + \exp\left(\frac{r-R}{a}\right)}. \tag{6}$$

However, the two models make slightly different assumptions for the nuclear radius R and the diffuseness parameter a. The VENUS parameterization is

$$\begin{aligned} R_{\mathrm{VEN}} &= (1.19A^{1/3} - 1.61A^{-1/3})\,\mathrm{fm} \\ a_{\mathrm{VEN}} &= 0.54\,\mathrm{fm} \end{aligned} \tag{7}$$

which results in $R_{\mathrm{VEN}} \approx 6.78$ fm for a lead nucleus. The radius parameter in FRITIOF for nuclei with $A > 16$ is calculated as

$$\begin{aligned} R_{\mathrm{FRI}} &= r_0 \cdot A^{1/3} \quad \text{with} \\ r_0 &= 1.16 \cdot (1 - 1.16A^{-2/3})\,\mathrm{fm}. \end{aligned} \tag{8}$$

This gives $R_{\mathrm{FRI}} \approx 6.65$ fm for lead nuclei. The diffuseness parameter a is taken to be slightly A-dependent in FRITIOF and lies in the range $0.47\,\mathrm{fm} - 0.55\,\mathrm{fm}$. For lead nuclei FRITIOF uses

$$a_{\mathrm{FRI}} = 0.545\,\mathrm{fm}. \tag{9}$$

Electron scattering experiments have shown, however, that the density distribution has a slightly more complicated structure[1]. For a comparison we will use a parameterization fitted to electron scattering data on ^{208}Pb presented in [28]:

$$\rho_{\mathrm{exp}}(r) = \rho_0 \cdot \frac{c_1 + c_2 r + c_3 r^2}{1 + \exp\left(\frac{r-R_{\mathrm{exp}}}{a_{\mathrm{exp}}}\right)} \tag{10}$$

with

$c_1 = 0.0633,\ c_2 = -0.002045\,\mathrm{fm}^{-1}, c_3 = 0.000566\,\mathrm{fm}^{-2}$

---

[1] Strictly this applies only to the charge distribution. The true nucleon distribution, especially in the inner part of the nuclei, is not experimentally accessible
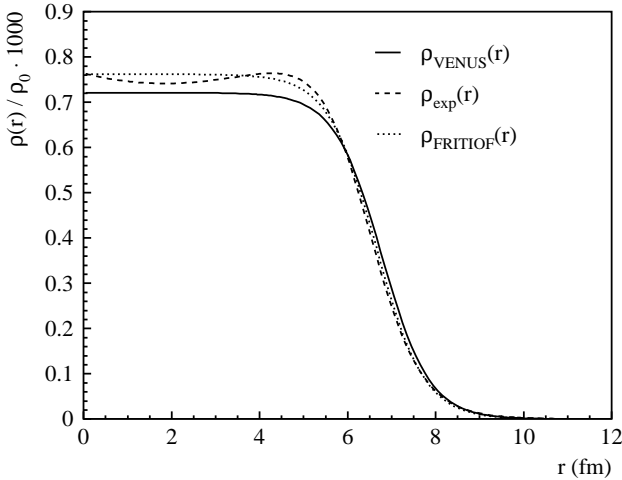
Fig. 15. Different nuclear density distributions used in the calculations of the number of participants and the number of collisions. The solid line shows the distribution implemented in the VENUS 4.12 Monte-Carlo model ((6) with the parameters (7)), the dashed line shows a parameterization of the charge distribution obtained from electron scattering (10) and the dotted line shows the density used in the FRITIOF model ((6) with the parameters (8) and (9))

and

$$R_{\exp} = 6.413 \, \text{fm}, \; a_{\exp} = 0.5831 \, \text{fm}.$$

The three different distributions are shown in Fig. 15. It can be seen that the overall agreement is quite good. The default distribution of VENUS has a slightly larger radius, while the parameterization of the experimental data shows small oscillations compared to the other two distributions.

With respect to the experimental resolution we have varied the energy resolution of the MIRAC calorimeter in the simulations. The measured values of the resolution [13] are for the electromagnetic section:

$$\frac{\sigma_{\text{em}}}{E} = \frac{17.9 \, \%}{\sqrt{E/\text{GeV}}} \tag{11}$$

and for the hadronic section:

$$\frac{\sigma_{\text{had}}}{E} = \frac{46.1 \, \%}{\sqrt{E/\text{GeV}}}. \tag{12}$$

This has been arbitrarily worsened to

$$\frac{\sigma_{\text{em,had}}}{E} = \frac{85 \, \%}{\sqrt{E/\text{GeV}}} \tag{13}$$

for both sections of the calorimeter.

For an accurate determination of the number of participants and the number of nucleon-nucleon collisions it is necessary that the experimental minimum bias threshold is reproduced in the simulation. In Sect. 2 we stated the two sources in the determination of the experimental minimum bias cross-section: the error of the target thickness and the error due to subtraction of interactions outside the

Table 1. The number of participants and binary collisions for different centrality classes obtained with the measured transverse energy in Pb+Pb collisions calculated from VENUS and FRITIOF (see text)

% of c.s.	E_T^{min} (GeV)	N_{part} VENUS	N_{coll}	N_{part} FRITIOF	N_{coll}
1	398.8	380.7	810.7	380.3	717.4
5	355.8	355.8	739.4	355.4	662.3
10	313.1	310.9	621.7	313.0	562.9
15	275.2	269.7	518.5	270.0	469.9
20	239.8	233.3	429.5	232.8	389.4
25	208.0	202.0	357.2	201.0	324.5
30	179.2	174.2	293.6	172.3	264.7
35	153.7	149.3	240.1	147.3	218.6
40	130.3	128.2	197.3	125.7	177.2
45	109.7	109.3	159.4	105.4	141.8
50	91.2	91.4	126.1	89.2	114.6
55	74.8	76.2	99.2	73.3	89.2
60	60.4	62.6	76.7	60.3	69.1
65	47.9	51.2	59.1	49.2	53.4
70	37.0	41.3	44.8	39.1	39.6
75	27.9	32.4	32.6	30.9	29.8
80	20.5	25.5	24.2	23.9	21.5
85	14.7	19.5	17.3	17.8	15.1
90	10.3	14.6	12.1	13.1	10.4
95	6.9	10.9	8.6	9.8	7.4
100	0.0	8.3	6.2	7.5	5.4

target. In our approach of calculating the number of participants and nucleon-nucleon collisions we define centrality classes based on the simulated E_T (in case of the N_{ch} scaling analysis) which correspond to the same absolute cross-sections as the respective classes for the measured E_T. The uncertainty of the minimum bias cross-section due to the error of the target thickness therefore directly leads to an error of the N_{part}-values which affects the entire centrality range. However, the uncertainty in the correction for interactions outside the target affects the experimental $d\sigma/dE_T$ distribution only in the peripheral range. More precisely, since the maximum E_T measured in target-out events is around 75 GeV, according to Table 1 only the range $N_{part} < 50$ is affected.

The measured target thickness is $213 \pm 3 \, \mu$m. The uncertainty of the target thickness contributes a relative error of roughly 1.5% to the error of the experimental minimum bias cross section. In order to check the influence on the extracted scaling exponent we arbitrarily increase the minimum bias threshold in the simulation by roughly 2% to $\sigma_{mb}^{sim} = 6386 \, \text{mb}$. We have furthermore checked the error of α_p due to the uncertainty of the minimum bias cross section that relates to the subtraction of non-target contributions. To do this, we have used an E_T distribution without correction for reactions outside the target to translate the experimental E_T cuts into cross section
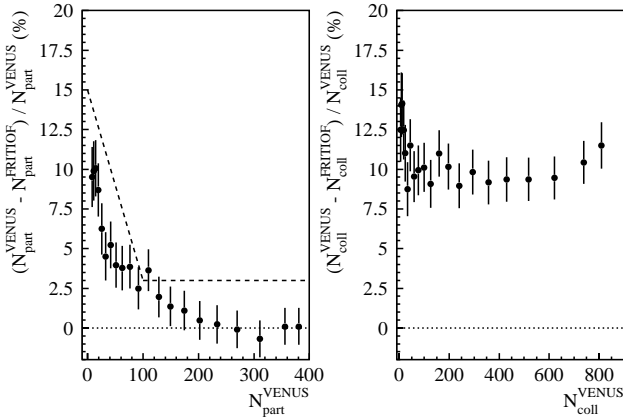
Fig. 16. Relative difference of the number of participants (left) and the number of nucleon-nucleon collisions (right) calculated with VENUS (calculation A) and FRITIOF (calculation F). The dashed line on the left plot indicates the assumed uncertainty of the participant scale that is used in the calculation of the error bars in Fig. 7

Table 2. Influence of different model assumptions on the extracted exponents α_p and α_c which describe the scaling of the charged particle yield with N_{part} and N_{coll} according to (1). In addition to the scaling exponents we quote the proportionality constants for the scaling with N_{part} (c_p) and N_{coll} (c_c) for each calculation. The full centrality range was used in the fit of (1) to the measured charged particle yields

Calculation	c_p	α_p	c_c	α_c
A	0.83	1.08	1.94	0.83
B	0.88	1.07	2.15	0.81
C	0.86	1.07	1.99	0.83
D	0.98	1.05	2.13	0.83
E	0.87	1.07	2.01	0.82
F	0.97	1.05	2.13	0.83

cuts. The apparent minimum bias cross section for this E_T distribution was $\sigma_{mb} = 6530$ mb.

The different calculations of the number of participants and collisions are summarized in the following list:

A VENUS 4.12 calculations using the standard settings for the density distribution, the experimental resolution and the minimum bias cross section.

B VENUS 4.12 calculations as in case Appendix A: with a modified density distribution according to (10).

C VENUS 4.12 calculations as in case Appendix A: with a modified MIRAC resolution.

D VENUS 4.12 calculations as in case Appendix A: with an a minimum bias cross section increased to $\sigma_{mb}^{sim} = 6386$ mb.

E VENUS 4.12 calculations with cross section cuts derived from an experimental E_T-spectrum that was not corrected for interactions outside the target (apparent minimum bias cross section: $\sigma_{mb} = 6530$ mb).

F FRITIOF calculations using standard settings as in calculation A.

As an example, the number of participants and collisions from calculation A and F are compared in Fig. 16. In peripheral Pb+Pb reactions VENUS gives up to 10% more participants than FRITIOF whereas in central reactions both simulations yield almost identical results. Almost independent of centrality the number of collisions from VENUS is roughly 10% higher than the FRITIOF result. The results of calculation A and F together with the experimental E_T intervals are given in Table 1.

For the case of the N_{ch} scaling the impact of the different model assumptions on the extracted scaling exponents α is summarized in Table 2. Considering the scaling with the number of participants we take the average of the α_p values from calculations A, B and F as our final result since all three calculations are based on reasonable assumptions. The maximum difference of 0.03 between the α_p values from these calculations is taken as one contribu-

tion to the systematic error. By adding the deviations of the results from calculations C, D and E from the mean value 1.07 in quadrature we estimate the total systematic error of α_p related to the uncertainty of the number of participants to be 0.036. The same prescription yields an uncertainty of 0.024 for the exponent α_c that described the scaling with the number of binary nucleon-nucleon collisions.

References

1. D. Antreasyan, et al. Phys. Rev. D **19**, (1979) 764
2. A. Krzywicki et al., Phys. Lett. **B 85**, (1979) 407
3. M. Lev, B. Petersson, Z. Phys. C **21**, (1983) 155
4. A. Bialas, A. Bleszynski, W. Czyz, Nucl. Phys. B **111**, (1976) 461
5. WA80 collaboration, R. Albrecht et al., Phys. Rev. C **44**, (1991) 2736
6. D.K. Srivastava, K. Geiger, preprint nucl-th/9808042
7. J. Sollfrank et al., Nucl. Phys. A **638**, (1997) 399c
8. WA98 collaboration, M. Aggarwal et al., Phys. Rev. Lett. **81**, (1998) 4087
9. WA98 collaboration, M. Aggarwal et al., Phys. Rev. Lett. **84**, (2000) 578 (erratum to M. Aggarwal et al., Phys. Rev. Lett. **81**, (1998) 4087)
10. NA50 collaboration, M.C. Abreu, et al., Nucl. Phys. A **638**, (1997) 261c
11. NA50 collaboration, M.C. Abreu, et al., Phys. Lett. **B 410**, (1997) 327
12. R.Vogt, Phys. Lett. **B 430**, (1998) 15
13. T.C. Awes et al., Nucl. Instr. and Meth. A **279**, (1989) 479
14. W.T Lin et al., Nucl. Instr. and Meth. A **389**, (1997) 415
15. R. Brun et al., GEANT3, CERN/DD/cc/84-1
16. K. Werner, Phys. Rep. **232**, (1993) 87
17. WA80 collaboration, R. Albrecht et al., Z. Phys. C **55**, (1992) 539
18. WA98 collaboration, M. Aggarwal et al., Phys. Lett. B **458** (1999) 422
19. K. Reygers, doctoral thesis, University of Münster, Germany (1999)

20. WA98 collaboration, M. Aggarwal et al., Phys. Rev. Lett. **85**, (2000) 3595
21. WA98 collaboration, M. Aggarwal et al., nucl-ex/0006007, submitted to Phys. Rev. C
22. C. DeMarzo et al., Phys. Rev. D **26**, (1982), 1019
23. C.Y. Wong, Z.D Lu, Phys. Rev. D **39**, (1989) 2606
24. C.Y. Wong, Phys. Rev. D **32**, (1985) 94
25. C.Y. Wong, Introduction to High-Energy Heavy-Ion Collisions, World Scientific Co., Singapore (1994), 280–281
26. J.E Elias et al., Phys. Rev. Lett. **41**, (1978) 285
27. C.Y. Wong, Phys. Rev. D **30**, (1984) 961
28. B. Frois et al., Phys. Rev. Lett. **38**, (1977) 152
29. H. Pi, Comput. Phys. Commun. **71**, (1992) 173